# Overvoltage Limitation Method of an Offshore Wind Farm with DC Series-Parallel Collection Grid

Haibo Zhang, François Gruson, Diana M. Flórez Rodriguez, and Christophe Saudemont

***Abstract*—This paper describes the characteristics of a series parallel wind farm (SPWF) topology and investigates the control strategy to ensure its safe operation. The SPWF was found to have advantages over other pure dc wind farm architectures in terms of lower construction cost and lower power losses in the collection system. However, unbalance power productions among the wind turbines cause the variations of their output voltages, which may endanger the safe operation of the entire wind farm. This paper proposes a global control strategy that prevents wind turbines from operating above their overvoltage capabilities. With an active participation of the onshore converter, the proposed strategy allows maximum power point tracking (MPPT) of the wind turbines. The practical limitations of this strategy are discussed and improvements are given. The feasibility of the proposed method is validated in a simulation of 300 MW wind farm developed in EMTP-RV.**

***Index Terms*—dc offshore wind farm, HVDC transmission, modular multilevel converter (MMC), overvoltage limitation.**

## I. Introduction

THE exploitation of far-offshore wind energy introduces new challenges in offshore power transmission and ac grid integration. It has been found unsuitable to use HVAC for long distance submarine transmission, because the reactive power generated by ac cables can considerably undermine its transmission capability [1]. Consequently, high voltage dc (HVDC) technology is dominating in large long-distance offshore projects.

Conventional point-to-point HVDC transmission increases the power conversion stages compared to HVAC, which indicates higher power conversion losses and higher installation and maintenance costs [2]. Correspondingly, potential efficiency improvement and cost reduction reside in eliminating large power transformers, power converters and platforms. This leads to recent investigations on pure dc offshore wind farm with dc collection and transmission systems [3], [4].

Most pure dc configurations simply replace the power transformers in the wind turbine and in the offshore substation with dc/dc converters [5]. These configurations do not reduce the power conversion stages. Instead, the focus is placed on improving the power conversion efficiency by new dc/dc converter designs [6]–[10].

Through recent studies, a promising solution to reduce the power conversion stages of the pure dc configurations is to series connect wind turbines with dc output in a cluster. The cluster establishes the HVDC transmission voltage directly at the collection grid side, so that the centralized offshore converter and its platform are not necessary. The wind turbines in the cluster must share a same cluster current, which gives rise to a group of series topologies using thyristor based HVDC [11]. A HVDC link using a current source inverter (CSI) at onshore and diode rectifiers at offshore is studied in [12]. A similar thyristor based configuration using simple buck choppers at the wind turbine outputs is proposed in [13]. The main disadvantages of these configurations are the limitations of line commutated thyristors [14], and the usage of transformer-less converters in the wind turbines, so that there is no galvanic isolation between the wind turbine and the HVDC transmission system.

Another potential method to series connect the wind turbines is to use voltage source converter (VSC) based HVDC configuration, which is firstly proposed in [4] called series parallel wind farm (SPWF) topology, and this is the method considered in this paper. The studied power generation and transmission system is shown in Fig. 1. The HVDC voltage is controlled by an onshore multilevel modular converter (MMC). In the collection grid, full bridge dc/dc converters are used to step up the low wind turbine generator side dc voltage to medium level. In this paper, it is assumed that the intermediate transformer in the dc/dc converter also serves to provide galvanic isolation for the wind turbine. However, the galvanic isolation level of the first and last wind turbines to the common mode voltage, equivalent to half of the HVDC transmission voltage, still remains a practical challenge to the academic and industrial communities. This paper focuses on the operation issues of this MMC-HVDC based SPWF, aiming to increase the power availability of this topology.

The comparison of the SPWF with other dc configurations regarding power losses, costs of components, and power availability/reliability are studied in [6], [15]. The clear advantages of the SPWF are lower collection grid losses, and lower construction and maintenance costs, thanks to the elimination of the offshore converter and platform. However, the MMC-controlled HVDC voltage imposes overvoltage on certain series connected wind turbines operating in uneven wind conditions. If the overvoltage surpasses a permitted limit, it may lead to cascade failure of the entire cluster. A solution is suggested in [4] to utilize an output voltage limitation controller which actively reduces the power production of overvoltage units. However, this leads to undesired power losses. Another solution proposed in [16] can mitigate the overvoltage level by topology modification. The modified collection grid allows currents to flow into adjacent clusters.

H. Zhang, F. Gruson, Diana M. Flórez R. and C. Saudemont are with Univ. Lille, Arts et Metiers ParisTech, Centrale Lille, HEI, EA 2697 - L2EP - Laboratoire d'Electrotechnique et d'Electronique de Puissance, F-59000 Lille, France.

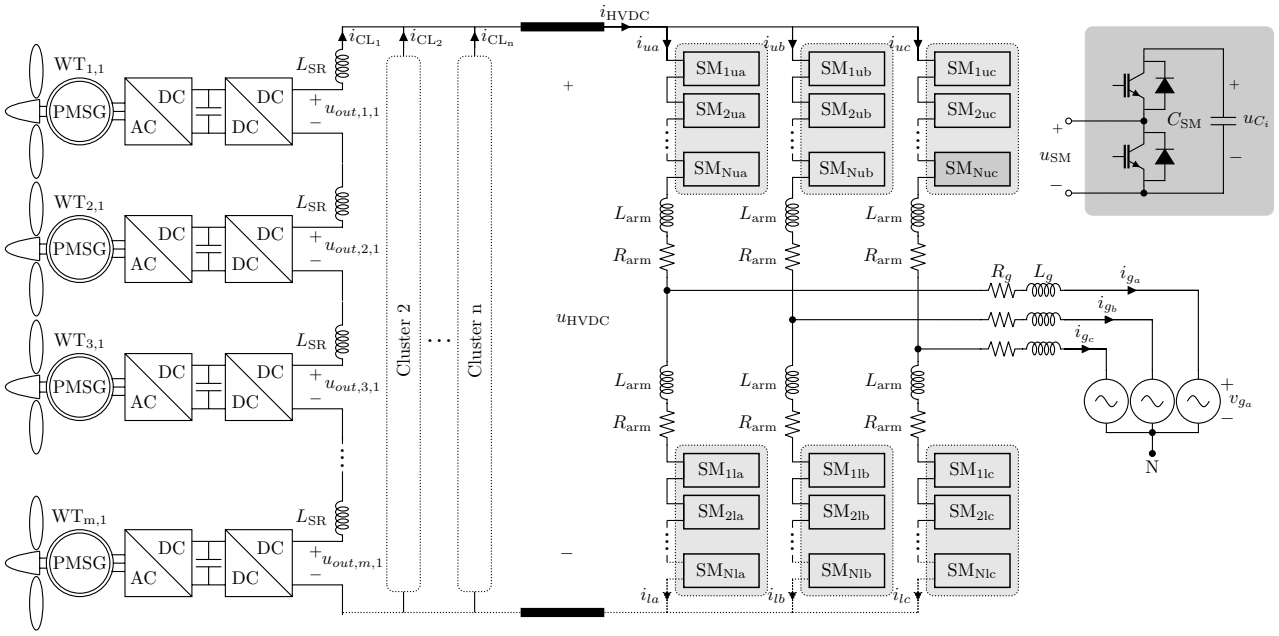


Fig. 1: MMC based dc SP offshore wind energy generation system.

But the substantial investment on extra switch gears and overrated cables is not considered in the author's cost analysis.

This paper, therefore, proposes a novel overvoltage limitation strategy which requires communication between wind farm and onshore converter, and active participation of the onshore converter in limiting the wind turbines output voltages. Section II of this paper describes the studied system. The proposed limitation strategy, practical limitations and improvements are presented in section III. Section IV deals with the corresponding control systems. In Section V, a simulation on a 300 MW wind farm has been developed in EMTP-RV [17] to investigate the feasibility of proposed control strategy. The conclusion is made in Section VI.

## II. System description

Fig. 1 shows the entire studied system in which a $m \times n$ SPWF is integrated to the onshore grid by MMC based HVDC technology. The collection grid of the SPWF is composed of $n$ parallel connected clusters. In each cluster, $m$ wind turbines are connected in series to establish the HVDC voltage. The MMC consists of six arms of cascaded submodules (SMs). A SM with half bridge topology is shown in the figure.

The whole system features the modular multilevel concept at both offshore and onshore sides. But there is substantial difference between the SPWF and MMC from the energy distribution point of view. Energy balancing among the SM capacitors is one of the main problems of MMC. The balancing capacitor algorithm (BCA) is implemented, so that the SM capacitor voltages are regulated equally [18]. However, the power of each wind turbine in the SPWF depends on the wind speed, which is not controllable. Unequal power production among the units leads to uneven allocation of output voltage across the dc/dc converters. Therefore, the output dc/dc converters are required of variable output voltage capability, and thus, variable input-output transformation ratio. The significance of this characteristics will be further addressed.

### A. SPWF main components

The wind turbines employ permanent magnetic synchronous generators (PMSGs) and fully rated power rectifiers. The dc/dc converter steps up the low intermediate dc link voltage to medium voltage. The most adopted dc/dc converters with insulation transformers in the literature are: full bridge converter (FBC) [19], single active bridge (SAB) [20], dual active bridge converter (DAB) [21] and series resonant converter (SRC) [22]. In this paper, the FBC is adopted for two reasons: 1) the buck type converter ensures a continuous flow of the cluster current; 2) the ability to vary transformation ratio. The FBC is shown in Fig. 2a and corresponding duty cycle control block is shown in Fig. 2b. The outer loop of the control aims to maintain the intermediate dc link voltage $u_{in}$ to be constant, while the output voltage of the FBC is not controlled.

To prevent the failure of a single unit from triggering cascade failure in the cluster, a bypass protection system is needed to bypass the fault wind turbine. Two bypass solutions are therefore proposed. The first solution is shown in Fig. 3a. The dc breakers at the output of the dc/dc converter directly cut off the entire wind turbine from the cluster. Simultaneously, a connector switches on to provide a current path. The second solution is to use the diode bridge of the FBC as the cluster current path, as shown in Fig. 3b. When the internal fault is detected, the IGBTs are kept at off-state. The output capacitor voltage gradually decreases to zero.

The smoothing reactor in the cluster is designed to a value big enough to limit the gradient of current boost $\Delta i_{\mathrm{HVDC}}/\Delta t$ during critical HVDC faults. The smoothing reactor is split evenly to as many parts as the number of wind turbines, and

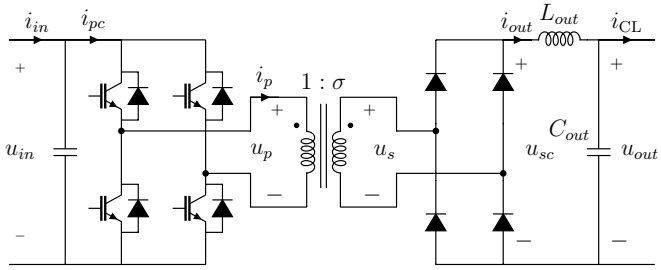


(a) Converter circuit

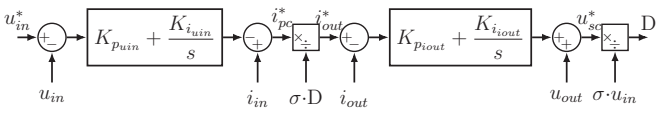


(b) Dual-loop control blocks

Fig. 2: Full bridge DC/DC converter and control blocks.

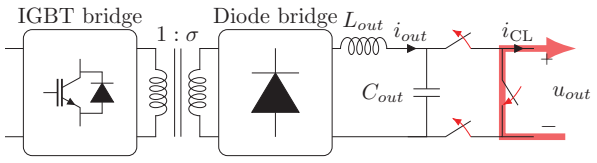


(a) Solution 1: using dc breakers

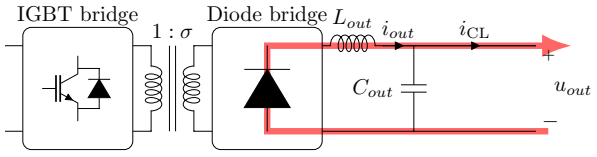


(b) Solution 2: using diode bridge

Fig. 3: Bypass protection solutions.

thus each part $L_{\text{SR}}$ is small enough to be placed inside the wind turbine tower, as shown in Fig. 1.

### B. Steady state operation principles

In the collection system, the HVDC link voltage is regulated by the onshore MMC, while the wind turbine output voltage is not individually controlled. Assuming that the power electronics devices in wind turbines are ideal and have infinite voltage and current capabilities, the operation of wind turbines follows the Kirchhoff Circuit Laws. Output voltage of the x$^{\text{th}}$ wind turbine located in cluster y, $\text{WT}_{\text{x,y}}$, is calculated as:

$$u_{out,x,y} = u_{\text{HVDC}} \frac{p_{out,x,y}}{\sum_{x=1}^{m} p_{out,x,y}} = u_{\text{HVDC}} \frac{p_{out,x,y}}{p_{\text{CL},y}} \tag{1}$$

$$i_{\text{CL},y} = \frac{p_{\text{CL},y}}{u_{\text{HVDC}}} = \frac{p_{out,x,y}}{u_{out,x,y}} \tag{2}$$

where the wind turbine power production and output voltage are represented by $p_{out,x,y}$ and $u_{out,x,y}$. $p_{\text{CL},y}$ and $i_{\text{CL},y}$ are the power production and current of cluster $y$, respectively.

Equation (1) gives the steady state output voltage of a wind turbine in the SPWF. It implies that the output voltage depends not only on its own power, but also on the power of its cluster. It has been mentioned that the output dc/dc converter regulates its input dc link voltage instead of its output voltage. The output voltage variation is illustrated in Fig. 4. When the wind turbine power generation is higher or lower than the average power in the cluster, the power unbalance is reflected by the unmatched currents at both sides of the wind turbine output capacitor. The stiff current $i_{out}$ charges or discharges the output capacitor, which consequently results in the increase or decrease of the output voltage $u_{out}$, as shown in Fig. 4.

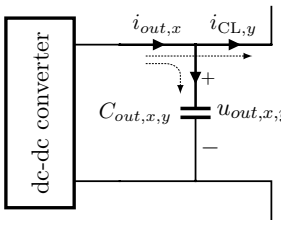


(a) $p_{out,x,y} > p^{ave}_{\text{CL},y}$

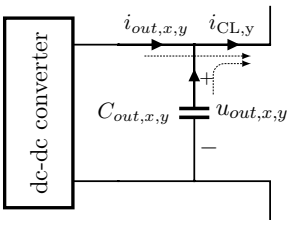


(b) $p_{out,x,y} < p^{ave}_{\text{CL},y}$

Fig. 4: Variation of output voltage due to power imbalance between the wind turbine and average level of the cluster.

### C. Definition of overvoltage

The HVDC voltage is regulated to $m$ times the wind turbine nominal voltage $U_{out,nom}$ by the onshore MMC. Due to the wind speed variation, certain wind turbines output voltage may rise above its nominal value, and these particular units are in *overvoltage*. Bypassing fault wind turbines also pushes the remaining fault-free units to operate in *overvoltage*. The maximum voltage level which a wind turbine converter can support is its *overvoltage capability* $U_{limit}$. The ratio between the overvoltage capability and the nominal output voltage is denoted as $\alpha$.

A higher overvoltage capability permits a larger power disparity in the cluster. Nevertheless, physically expanding the size of converter is neither economical nor practical. For these reasons, *overvoltage limitation control* should be developed to prevent wind turbine from operating above their permitted overvoltage capability.

## III. Overvoltage Limitation Control

As mentioned in the introduction, a local overvoltage limitation method is proposed in [4]. When the output voltage reaches the overvoltage capability, an output voltage limitation controller is triggered to prevent the output voltage from increasing, by the means of reducing the wind turbine power production. The control diagram is shown in Fig. 5. The output of the voltage limitation controller is taken as a compensation torque $T_{em,com}$ to the inner current controller of the rectifier. The value of this torque will always be negative, and thus the torque reference for the inner current loop reduces. The compensation torque disables the MPPT of the wind turbine, leading to wind power curtailment.

In this paper, a new solution named as global overvoltage limitation strategy is proposed, which ensures both the safe

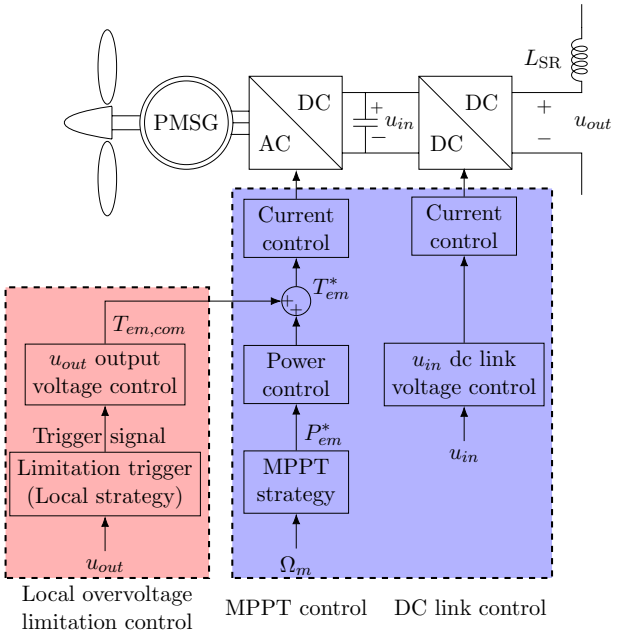


Fig. 5: Local overvoltage limitation control diagram.

operation of each wind turbine within its overvoltage capability and MPPT.

### A. Basics of the global overvoltage limitation strategy

The proposed global control strategy divides the wind farm operation into two working modes: normal mode and overvoltage limitation mode. In normal mode, the wind turbines output voltages are allowed to vary under their overvoltage capabilities $U_{limit}$. The reference HVDC voltage $u^*_{\text{HVDC}}$ of the MMC is constant, equivalent to the sum of wind turbines nominal output voltages $U_{out,nom}$:

$$u^*_{\text{HVDC}} = mU_{out,nom} \tag{3}$$

When the output voltage of any wind turbine reaches its overvoltage capability level, the onshore converter enters into voltage limitation mode. The HVDC voltage is regulated to the level which can ensure the output voltage of the wind turbine with the maximum power production in the wind farm to stay under the the overvoltage limit:

$$u^*_{\text{HVDC}} = \min\left(U_{out,nom}\frac{p_{\text{CL},y}}{\max(p_{out,x,y})}\right). \tag{4}$$

The control scheme of the global control and corresponding controller references of the MMC are depicted in Fig. 6.

The bypassed fault unit can be regarded as a wind turbine with zero power production and therefore its output voltage equals to zero. The corresponding cluster is reduced to a series connection with $(m-k)$ units, $k$ is number of bypassed units. In this case, all the remaining units in the cluster are operated at overvoltage, if the HVDC voltage remains at $mU_{out,nom}$. Even all the rest units in the cluster produce nominal power, their output voltages are clamped to $\frac{m}{m-k}U_{out,nom}$. With this clamped voltage as base voltage, there is very little margin

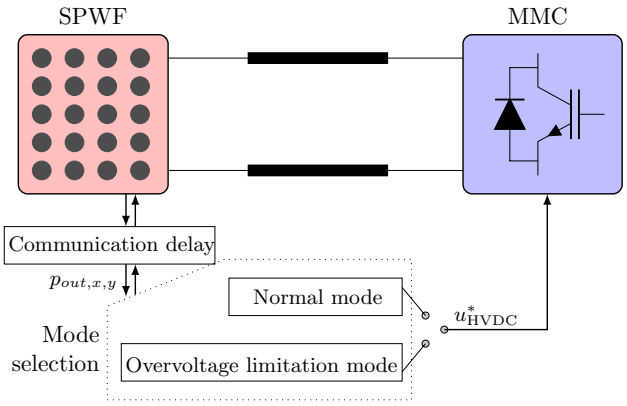


Fig. 6: Global control scheme of the SPWF-MMC HVDC.

left for the voltage variation. It is then proposed to reduce the base HVDC voltage to:

$$u^{\text{base}}_{\text{HVDC}} = \frac{m-k}{m}U_{out,nom}. \tag{5}$$

The overvoltage limitation strategy obeys the above working modes based on this reduced HVDC voltage.

The advantage of this strategy is that wind turbines do not need to reduce their own power production. Accurate information of all wind turbines operating condition is essential, which depends on data communication via the fibre optic cable embedded in the HVDC cables.

### B. Constraints of basic global strategy

It is important to note some practical limitations of the proposed global control strategy:

1) Communication delay and interruption
   The communication delay is of the order of several dozens of milliseconds. In large power systems such as in the Bonneville Power Administration system, the latency of fibre communication is reported as approximately 38 ms for one way [23]. The latency is caused by the fact that the electrical devices do not have inherent communication capabilities, and therefore they have to rely on embedded computer systems to serve as communication interfaces. The most significant delays during the process are the data acquisition delay, the packet processing and transmission delay [24]. In the SPWF, the MMC response time and capacitive HVDC cables also lead to the event responding delay.
2) Minimum allowable HVDC voltage level
   The second constraint is related to the practical limitations of the MMC. In order to prevent the diode bridge from forward bias and consequently lose the full control of the MMC, the HVDC voltage $u_{\text{HVDC}}$ should always be greater than the peak value of ac side phase-to-phase voltage:
   $$u^*_{\text{HVDC}} > \sqrt{6}V_g \tag{6}$$
   where $V_g$ is the RMS value of the grid phase-to-neutral voltage.

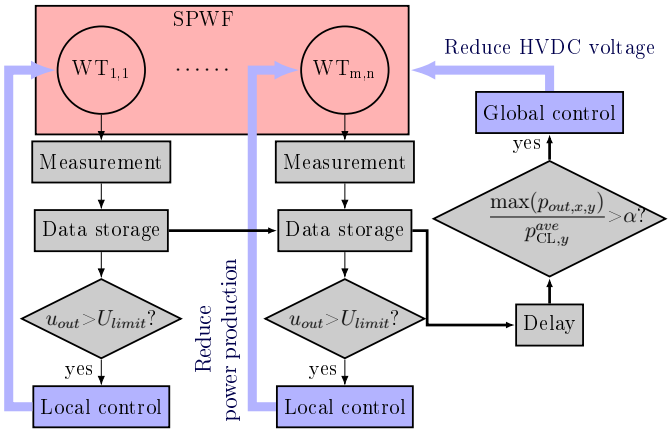


Fig. 7: Arrangement of global and local controls of the SPWF.

3) HVDC cables and onshore MMC losses
The proposed global control reduces the HVDC voltage, which definitely increases the HVDC cable current and cable power losses.
Increased HVDC current also has an influence on the conduction and switching losses of the semiconductors in the MMC. The MMC has a much lower switching frequency compared to a conventional 2-level or 3-level VSC. It is found in [25] that the biggest share of power losses presented in the MMC is the conduction losses of the semiconductors. Usually, one suggests that it is necessary to limit the RMS value of the currents flowing through the converters to limit their losses. However, reference [26] shows that the conduction losses of the MMC are not only related to the currents' RMS values, but also the waveforms of these currents and therefore the MMC control algorithms. Because the total losses in the MMC are very low (around 1% of the nominal power), the estimation of MMC losses is not studied in this paper.

### C. Optimal HVDC voltage

Due to the above issues of the global control, it is suggested that the local overvoltage limitation controllers be installed in the wind turbines. When the global control reaches the mentioned limitations, the local control should be activated to serve as complementary limitation controllers. To summarize, the two kinds of overvoltage limitation controls play different roles in the SPWF:

- The local overvoltage limitation control activates during the communication delay and communication interrupts. Furthermore, it serves as a back-up control for when the HVDC has been reduced to its minimum allowable level.
- The global control serves to limit the wind turbines output voltages without power curtailment by reducing the HVDC voltage. It is selected as the primary option for voltage limitation.

The process of controlling the series wind farm by these two methods is illustrated in Figure 7.

The proposed global control increases the power production of the wind farm, comparing to the local control. However, the HVDC cable losses are also increased. This leads to an investigation of the optimal HVDC voltage level, which enables the onshore side to receive maximum power from the offshore side:

- On one hand, if only local control strategy is applied, this situation causes the maximum wind turbine power curtailment and the minimum cable losses.
- On the other hand, if only the global control is applied, this situation causes the maximum cable losses and the minimum wind turbine power curtailment.

As a result, the optimal voltage $\hat{u}^{opt}_{\text{HVDC}}$ has a compromised level, which must drop in the range:

$$\hat{u}^{gctl}_{\text{HVDC}} \leq \hat{u}^{opt}_{\text{HVDC}} \leq U_{\text{HVDC},nom} \tag{7}$$

where the hat $\hat{}$ denotes the variables at a reduced HVDC voltage level. $\hat{u}^{gctl}_{\text{HVDC}}$ is the reduced HVDC voltage if only the global strategy is applied, $U_{\text{HVDC},nom}$ is the nominal HVDC voltage.

In order to find this optimal voltage level, we decrease the HVDC voltage gradually, and then calculate the instant wind farm power production $\hat{p}_{\text{WF}}$ at each HVDC voltage level (note that the wind farm power production is partially reduced due to the accompanied local limitation controllers), as well as the cables losses $\hat{p}_{\text{cable}}$. At each voltage level, the subtraction of the wind farm power production and the cables power losses is the amount of power received at onshore:

$$\hat{p}_{\text{received}} = \hat{p}_{\text{WF}} - \hat{p}_{\text{cable}} \tag{8}$$

### D. Case study

To illustrate the above method to find the optimal HVDC voltage, a $20 \times 1$ SPWF is used for example. The nominal wind turbine output power $P_{out,nom}$ and voltage $U_{out,nom}$ are 5 MW and 32 kV, overvoltage ratio $\alpha = 0.1$. For a practical comparison of the cables power losses and the power curtailment due to local control, the commissioning Dolwin1 project is taken as reference. The power transmission length is 165 km. HVDC transmission voltage is $\pm$320 kV. The cables with copper conductor should have a section area of 85 mm$^2$ according to [27].

Assume that:

$$U_{out,nom} = P_{out,nom} = I_{\text{CL},nom} = 1 \text{ pu};\ U_{limit} = 1.1 \text{ pu}$$

The SPWF power instant production and output voltages without control strategy applied are:

$$\mathbf{p_{out}} = \begin{array}{c} \text{WT}_{x,1} \\ \text{1-4} \\ \text{5-8} \\ \text{9-12} \\ \text{13-16} \\ \text{17-20} \\ \hline \text{Sum} \quad 17.2 \text{ pu} \end{array} \begin{pmatrix} 1.00 \\ 1.00 \\ 0.80 \\ 0.80 \\ 0.70 \end{pmatrix} \quad \mathbf{u_{out}} = \begin{array}{c} \\ \\ \\ \\ \\ \hline 20 \text{ pu} \end{array} \begin{pmatrix} \boxed{1.1616} \\ \boxed{1.1616} \\ 0.9293 \\ 0.9293 \\ 0.8131 \end{pmatrix}$$

According to (1), $\text{WT}_{\text{1-8,1}}$ produce nominal power while their output voltage are greater than their capabilities 1.1 pu. By decreasing the HVDC voltage gradually and calculating the

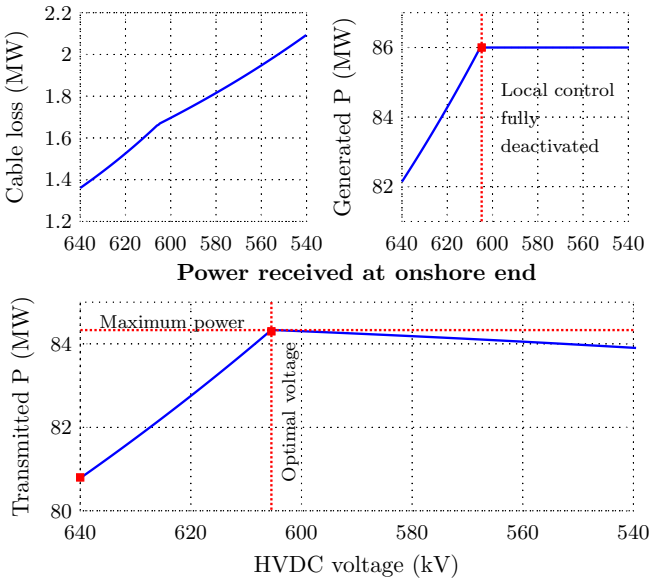


Fig. 8: Variation of the cable losses, SPWF generated power, and transmitted power to onshore.

received power at every HVDC voltage level, the variation of the received power is plotted in Figure 8.

At nominal HVDC voltage 640 kV, both the cable losses and the generated power from the SPWF are minimal. The local control needs to reduce the power production of $WT_{1\text{-}8,1}$ from 1 pu to 0.9036 pu, equivalent to 3.85 MW power curtailment. The power received at onshore is 80.8 MW. As expected, the cable losses increase as the HVDC voltage decreases. The received power peaks at 604.8 kV to 84.3 MW, 3.5 MW greater than using only local control strategy. Note that this voltage equals to the $\hat{u}^{gctl}_{\text{HVDC}}$ where the local control is fully deactivated. This indicates that in this case, in the whole range of $[\hat{u}^{gctl}_{\text{HVDC}}, U_{\text{HVDC},nom}]$, the reduction of voltage offers greater power generated by the SPWF than the cable losses. Further reducing the HVDC voltage below 604.8 kV, the cable losses increase while all wind turbines operate at MPPT, and therefore the power received at onshore side declines.

## IV. SPWF-MMC Models and Control Systems

Simulating the detailed EMTP-RV models of the wind turbine and onshore MMC is time consuming. Without losing generality, simplified models are adopted in the simulation: 1) a simplified wind turbine model with basic wind power conversion, dc/dc converter is fundamental to study the operating principles and characteristics of a SPWF with a number of units; 2) a simplified MMC model with dynamics and stored energy in each arm is necessary to realize the global control.

### A. Wind turbine generation system

This paper assumes that in normal mode, the PMSG wind turbine is controlled ideally to operate at MPPT. Based on this assumption, a simplified series wind turbine model can be created as shown in Fig. 9. The dc link voltage is controlled to be constant by the dc/dc converter, and thus the variation of the

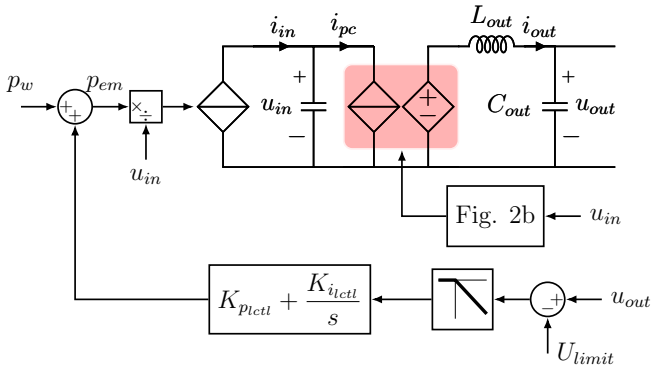


Fig. 9: Simplified wind turbine model with local overvoltage limitation controller.

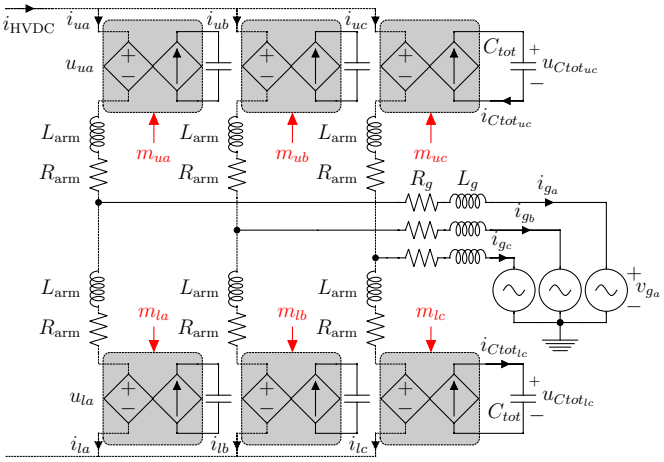


Fig. 10: MMC arm average model.

electromagnetic power $p_{em}$ is reflected as current variation of the controlled current source $i_{in}$. The dc/dc converter control follows the dual loop control described in Fig. 2b. The local overvoltage limitation control is represented by an negative input power compensation. In normal operation, the output voltage is lower than the overvoltage limitation, and thus the input to the output voltage limitation PI controller is always 0. As the output voltage reaches the limitation, this controller is activated. A negative compensation is added to the maximum extractable power $p_w$, and therefore $p_{em}$ decreases.

### B. Multilevel modular converter

In the literature, there exist several types of MMC models. This paper adopts the MMC arm average model, which assumes that all SM capacitor voltages are balanced. Although in this model the information of the switching states is lost, the dynamics and stored energy in each arm are retained [28]. Correspondingly, the low level control of MMC SMs is not considered. Only the high level control regarding to the MMC currents, voltages and stored energy is given.

The N+1 level detailed MMC shown in Fig. 1 can be reduced to the average model shown in Fig. 10. The equivalent MMC arm capacitance, referring to $C_{tot}$, equals to the sum of all SM capacitors $C/N$. By defining the duty cycle $m = n/N$

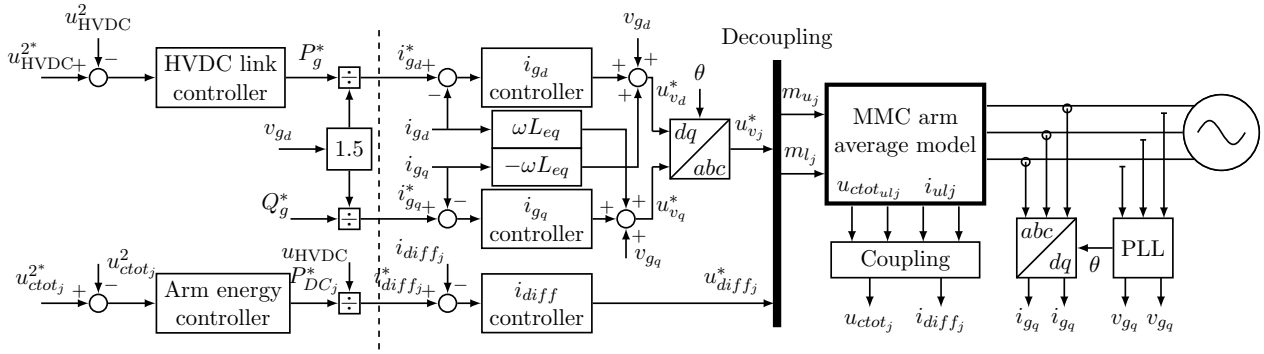


Fig. 11: High level control structure of MMC for HVDC voltage control.

with $n$ the number of active cells in the arm, new variables are deduced:

$$u_{ul_j} = m_{ul_j} u_{Ctot_{ulj}} \qquad i_{Ctot_{ulj}} = m_{ul_j} i_{ul_j} \tag{9}$$

where the subscripts $u$ and $l$ represent the upper arm and the lower arm, and $j$ referring to three phases $a$, $b$, $c$.

By performing the following variables changes,

$$u_{diff_j} = \frac{u_{u_j} + u_{l_j}}{2} \quad u_{v_j} = \frac{u_{l_j} - u_{u_j}}{2} \quad i_{diff_j} = \frac{i_{uj} + i_{lj}}{2}$$

$$L_{eq} = L_g + \frac{1}{2} L_{arm} \quad R_{eq} = R_g + \frac{1}{2} R_{arm}$$

the system can be decoupled to a dc part and an ac part (in dq reference frame) as:

$$\frac{u_{\text{HVDC}}}{2} - u_{diff_j} = L_{arm} \frac{di_{diff_j}}{dt} + R_{arm} i_{diff_j} \tag{10}$$

$$u_{v_d} - v_{g_d} = L_{eq} \frac{di_{g_d}}{dt} + R_{eq} i_{g_d} - \omega_g L_{eq} i_{g_q} \tag{11}$$

$$u_{v_q} - v_{g_q} = L_{eq} \frac{di_{g_q}}{dt} + R_{eq} i_{g_q} + \omega_g L_{eq} i_{g_d} \tag{12}$$

Neglecting the energy stored in the inductances, power exchange between the dc side and the ac side of the MMC in one phase induces the instantaneous energy change in one MMC phase (upper arm and lower arm):

$$p_{dc_j} - p_{ac_j} = \frac{dW_j^{\Sigma}}{dt} = \frac{1}{2} C_{tot} \Big( \frac{du^2_{Ctot_{uj}} + du^2_{Ctot_{lj}}}{dt} \Big). \tag{13}$$

Considering the HVDC cables as small capacitance:

$$\frac{1}{2} C_{dc} \frac{du^2_{\text{HVDC}}}{dt} = p_{\text{WF}} - p_{dc}. \tag{14}$$

The entire MMC control system is shown in Fig. 11. Thanks to the decoupling of the MMC system, the control of MMC can be separated into inner current loop and outer power (voltage) loop. This part of control system is similar to conventional 2-level VSC, and therefore will not be addressed in detail. The outer loop controllers are tuned 10 times slower than the inner loop. An unique feature of MMC is that the energy is distributed in the MMC arms. As a result, an extra arm energy control loop is added as shown in Fig. 11.

In the traditional two-level or three-level VSC, the dc bus voltage is directly established by the energy stored in dc link capacitor. In contrast, the energy stored in the arms of MMC is not directly linked to the dc bus voltage. By setting the energy reference of $u^2_{Ctot_{ulj}}$ to the square of the dc bus voltage $u^2_{\text{HVDC}}$, the MMC stored energy can be related to the dc bus as studied in [29]. Equation (14) becomes:

$$\frac{dW^{\Sigma}}{dt} = \frac{1}{2} C_{tot} \Big( 6 \frac{du^2_{\text{HVDC}}}{dt} \Big) = p_{dc} - p_{ac} \tag{15}$$

## V. Simulation results

The simulation of a $20 \times 3$ dc SPWF with the proposed control strategy and corresponding MMC control is fully developed and implemented in EMTP-RV. For the wind turbines, the nominal power and output voltage are 5 MW and 32 kV. The nominal HVDC voltage for the MMC is 640 kV. The overvoltage ratio $\alpha = 0.1$. The HVDC cables used in the simulation are 100 km WideBand models available in the EMTP-RV library. More parameters of SPWF, MMC and control systems are summarized in Tab. I and Tab. II.

### A. Wind speed variation

The first scenario simulates the functionalities of the overvoltage limitation control strategies when wind speed varies. The maximum extractable wind powers $p_w$ are plotted in Figure 12a. Wind turbines in the cluster 2 and 3 have identical wind speed variations as the units in the cluster 1. All units operate under their overvoltage capabilities until 4.6 s, as the power production unbalance increases, $\text{WT}_{\text{1-4,y}}$ reach their overvoltage capabilities.

In order to show the different behaviors of the local limitation control and the global limitation control, the communication delay is intentionally extended. Only the local limitation control is activated before 8 s and the global limitation is applied during 8 s to 10 s.

During 4.6 s to 8 s, the local limitation controllers in $\text{WT}_{\text{1-4,y}}$ reduce their power production to 4.65 MW as shown in Figure 12b. The local limitation controllers succeed in regulating the output voltages of $\text{WT}_{\text{1-4,y}}$ at 1.1 pu. The power received at onshore converter is -252.5 MW. The negative sign indicates that the power is transmitted from the HVDC system to the ac grid. From 8 s, the global limitation control is activated. The HVDC voltage is reduced to the optimal HVDC voltage $\hat{u}^{gctl}_{\text{HVDC}}$ 604.8 kV. The power productions of $\text{WT}_{\text{1-4,y}}$ are restored to

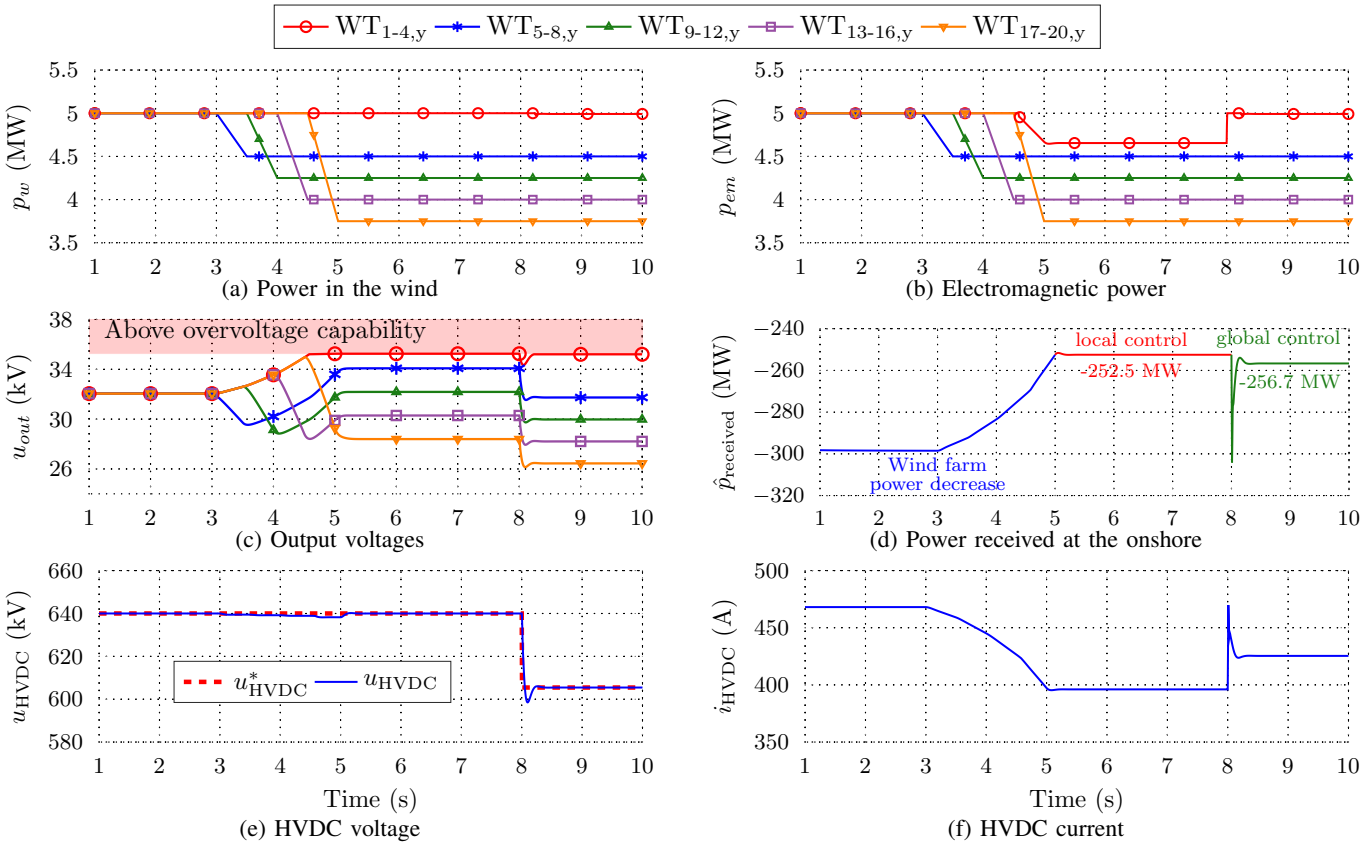


Fig. 12: Simulation results of the SPWF with local and global overvoltage limitation methods.

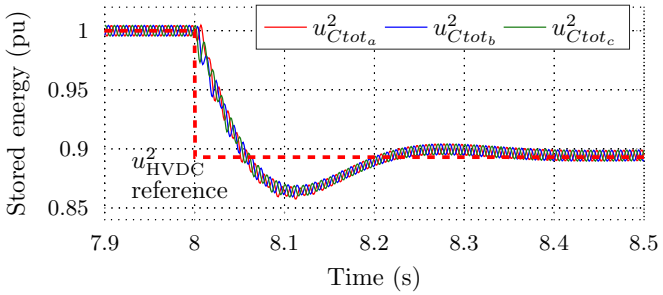


Fig. 13: MMC arm stored energy variation.

nominal power production because the local control is released owing to the reduction of HVDC voltage. As shown in Figure 12d, the received power at onshore steps up to -256.7 MW. Comparing these two overvoltage limitation strategies, 4.2 MW of power is recovered thanks to the proposed method.

The HVDC voltage and current are plotted in Fig. 12e and 12f. As explained in Subsection IV-B that, the energy reference of $u^2_{Ctot_{ulj}}$ is set to the square of the dc bus voltage $u^2_{\text{HVDC}}$, and therefore the MMC stored energy can be associated with the HVDC link. The variation of the MMC arm stored energy during the HVDC voltage reduction is plotted in Fig. 13. It can be noticed that the above description is validated.

### *B. One fault unit bypassed in the cluster 2*

In the second scenario all the wind turbines in the wind farm produce nominal power. One fault unit is bypassed in cluster 2 at 5 s. The communication delay is not intentionally increased.

Fig. 14a only shows the power variation of the entire cluster 1 (same as cluster 3) and cluster 2. At 5 s, cluster 2 suffers a sudden drop of power since one unit is bypassed. At almost the same time, the MMC regulates the HVDC voltage to 19 pu in order to remove the overvoltage imposed on all remaining wind turbines in the cluster 2. This results in a decrease of output voltage in the units located in cluster 1. Because the wind turbine output capacitors and the smoothing reactors construct a resonance circuit, the power unbalance between parallel connected clusters causes voltage oscillations across each unit. Fig. 14c presents the output voltage of $\text{WT}_{1,1}$ and $\text{WT}_{1,2}$. However, these oscillations do not occur on the transmission system. Fig. 14b and 14d plot the voltage and current of the HVDC transmission system. The energy only exchanges between the output capacitors and the smoothing reactors in the collection grid.

## VI. Conclusion

A dc collection grid with series connection of wind turbines allows a reduction of the power conversion stages, and consequently construction cost and power losses in the collection grid. A dc/dc converter with variable transformation ratio and a fault bypass system are essential for a wind turbine to operate

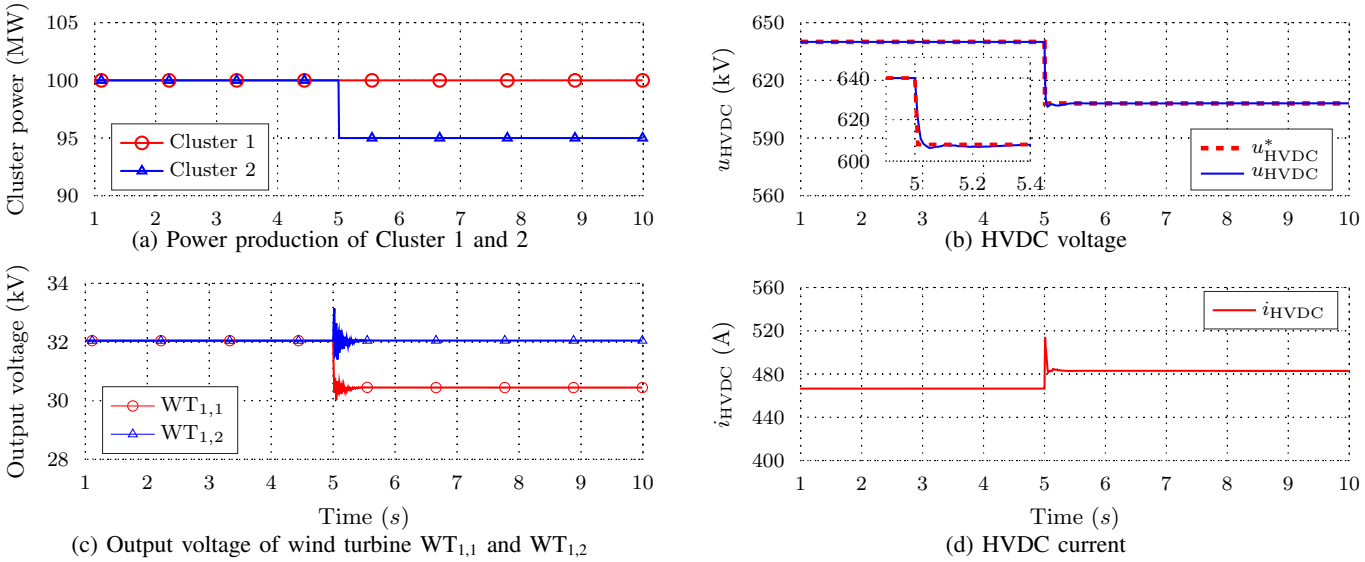


(a) Power production of Cluster 1 and 2

(b) HVDC voltage

(c) Output voltage of wind turbine $\mathrm{WT}_{1,1}$ and $\mathrm{WT}_{1,2}$

(d) HVDC current

Fig. 14: Simulation results of the SPWF when a fault unit is bypassed.

in the series topology which is connected to a VSC based HVDC system.

Unbalanced power production among wind turbines will cause variation of their output voltages, and may even render certain wind turbines unacceptable overvoltage. This paper compares two output overvoltage limitation methods. A local control method is fast but leads to wind power curtailment. On the contrary, the proposed global control method can ensure MPPT control for all wind turbines, but has some practical limitations regarding communication delay and increased cable losses. It is suggested in this paper to combine both control methods to ensure safe operation of all wind turbines. And it is found that the power gained by using the global control overwhelms the increased power losses in the cables. A series parallel offshore wind farm of 300 MW with 60 wind turbines is simulated in EMTP-RV, which validates the proposed control method by showing accordance results in the collection system and in the onshore MMC with the analysis.

## APPENDIX

TABLE I: System parameters

| Parameter | Notation | Value |
|---|---|---|
| DC link capacitor | $C_{in}$ | 10 mF |
| Output capacitor | $C_{out}$ | 293 $\mu$F |
| Output inductor | $L_{out}$ | 100 mH |
| Smoothing reactor per WT | $L_{\mathrm{SR}}$ | 5 mH |
| MMC arm resistor | $R_{arm}$ | 1.02 $\Omega$ |
| MMC arm inductor | $L_{arm}$ | 50 mH |
| Grid resistor | $R_g$ | 50 m$\Omega$ |
| Grid inductor | $L_g$ | 60 mH |
| Arm equivalent capacitor | $C_{tot}$ | 25 $\mu$F |

TABLE II: Controllers parameters

| Parameter | $K_p$ | $K_i$ |
|---|---|---|
| dc/dc current loop | 32 | 9000 |
| dc/dc voltage loop | 0.42 | 9 |
| Local voltage limitation loop | 7300 | $1.8 \times 10^5$ |
| PLL | 840 | $3.6 \times 10^5$ |
| Grid current loop | 100 | $2 \times 10^4$ |
| Differential current loop | 20 | 4500 |
| HVDC voltage loop | 0.004 | 0.08 |
| Stored energy loop | 0.001 | 0.023 |

## REFERENCES


[1] N. B. Negra, J. Todorovic, and T. Ackermann, "Loss evaluation of HVAC and HVDC transmission solutions for large offshore wind farms," *Electric Power Systems Research*, vol. 76, no. 11, pp. 916–927, Jul. 2006.

[2] P. Bresesti, W. L. Kling, R. L. Hendriks, and R. Vailati, "Hvdc connection of offshore wind farms to the transmission system," *IEEE Transactions on energy conversion*, vol. 22, no. 1, pp. 37–43, 2007.

[3] C. Meyer, M. Hoing, A. Peterson, and R. W. De Doncker, "Control and design of dc grids for offshore wind farms," *IEEE Transactions on Industry applications*, vol. 43, no. 6, pp. 1475–1482, 2007.

[4] S. Lundberg, "Wind farm configuration and energy efficiency studies - series DC versus AC layouts," Ph.D. dissertation, Chalmers University of Technology, Göteborg, Sweden, 2006.

[5] L. Max and S. Lundberg, "System efficiency of a dc/dc converter-based wind farm," *Wind Energy*, vol. 11, no. 1, pp. 109–120, 2008.

[6] N. Holtsmark, H. J. Bahirat, M. Molinas, B. A. Mork, and H. K. Hoidalen, "An all-dc offshore wind farm with series-connected turbines: An alternative to the classical parallel ac model?" *IEEE Transactions on industrial Electronics*, vol. 60, no. 6, pp. 2420–2428, 2013.

[7] A. Garcés and M. Molinas, "Coordinated control of series-connected offshore wind park based on matrix converters," *Wind Energy*, vol. 15, no. 6, pp. 827–845, 2012.

[8] D. Jovcic, "Step-up dc–dc converter for megawatt size applications," *IET Power Electronics*, vol. 2, no. 6, pp. 675–685, 2009.

[9] J. Robinson, D. Jovcic, and G. Joós, "Analysis and design of an offshore wind farm using a mv dc grid," *IEEE Transactions on Power Delivery*, vol. 25, no. 4, pp. 2164–2173, 2010.

[10] W. Chen, A. Q. Huang, C. Li, G. Wang, and W. Gu, "Analysis and comparison of medium voltage high power dc/dc converters for offshore

wind energy systems," *IEEE Transactions on Power Electronics*, vol. 28, no. 4, pp. 2014–2023, 2013.
[11] S. Nishikata and F. Tatsuta, "A new interconnecting method for wind turbine/generators in a wind farm and basic performances of the integrated system," *IEEE Transactions on Industrial Electronics*, vol. 57, no. 2, pp. 468–475, 2010.
[12] T. Kawaguchi, T. Sakazaki, T. Isobe, and R. Shimada, "Offshore-wind-farm configuration using diode rectifier with mers in current link topology," *IEEE Transactions on Industrial Electronics*, vol. 60, no. 7, pp. 2930–2937, 2013.
[13] E. Veilleux and P. W. Lehn, "Interconnection of direct-drive wind turbines using a series-connected DC grid," *IEEE Transactions on Sustainable Energy*, vol. 5, no. 1, pp. 139–147, Jan. 2014.
[14] N. Flourentzou, V. G. Agelidis, and G. D. Demetriades, "Vsc-based hvdc power transmission systems: An overview," *IEEE Transactions on power electronics*, vol. 24, no. 3, pp. 592–602, 2009.
[15] H. J. Bahirat, B. A. Mork, and H. K. Høidalen, "Comparison of wind farm topologies for offshore applications," in *Power and Energy Society General Meeting, 2012 IEEE*. IEEE, 2012, pp. 1–8.
[16] S. Chuangpishit, A. Tabesh, Z. Moradi-Sharbabk, and M. Saeedifard, "Topology design for collector systems of offshore wind farms with pure DC power systems," *IEEE Transactions on Industrial Electronics*, vol. 61, no. 1, pp. 320–328, Jan. 2014.
[17] J. Mahseredjian, S. Dennetière, L. Dubé, B. Khodabakhchian, and L. Gérin-Lajoie, "On a new approach for the simulation of transients in power systems," *Electric Power Systems Research*, vol. 77, no. 11, pp. 1514–1520, Sep. 2007.
[18] Q. Tu, Z. Xu, and L. Xu, "Reduced switching-frequency modulation and circulating current suppression for modular multilevel converters," *IEEE Transactions on Power Delivery*, vol. 26, no. 3, pp. 2009–2017, Jul. 2011.
[19] J. Sabate, V. Vlatkovic, R. Ridley, F. Lee, B. Cho *et al.*, "Design considerations for high-voltage high-power full-bridge zero-voltage-switched pwm converter," in *Proc. IEEE APEC*, vol. 90, 1990, pp. 275–284.
[20] R. W. De Doncker, D. M. Divan, and M. H. Kheraluwala, "A three-phase soft-switched high-power-density dc/dc converter for high-power applications," *IEEE transactions on industry applications*, vol. 27, no. 1, pp. 63–73, 1991.
[21] M. Kheraluwala, R. W. Gascoigne, D. M. Divan, and E. D. Baumann, "Performance characterization of a high-power dual active bridge dc-to-dc converter," *IEEE Transactions on industry applications*, vol. 28, no. 6, pp. 1294–1301, 1992.
[22] R. L. Steigerwald, "A comparison of half-bridge resonant converter topologies," *IEEE transactions on Power Electronics*, vol. 3, no. 2, pp. 174–182, 1988.
[23] H. Wu, K. S. Tsakalis, and G. T. Heydt, "Evaluation of time delay effects to wide-area power system stabilizer design," *IEEE Transactions on Power Systems*, vol. 19, no. 4, pp. 1935–1941, 2004.
[24] W. Wang, Y. Xu, and M. Khanna, "A survey on the communication architectures in smart grid," *Computer Networks*, vol. 55, no. 15, pp. 3604–3629, 2011.
[25] J. Freytes, F. Gruson, P. Delarue, F. Colas, and X. Guillaud, "Losses estimation method by simulation for the modular multilevel converter," in *Electrical Power and Energy Conference (EPEC), 2015 IEEE*. IEEE, 2015, pp. 332–338.
[26] F. Gruson, J. Freytes, S. Samimi, P. Delarue, X. Guillaud, F. Colas, and M. Belhaouane, "Impact of control algorithm solutions on modular multilevel converters electrical waveforms and losses," in *Power Electronics and Applications (EPE'15 ECCE-Europe), 2015 17th European Conference on*. IEEE, 2015, pp. 1–10.
[27] ABB, "HVDC light - cables submarine and land power cables," 2006. [Online]. Available: https://library.e.abb.com/public
[28] A. Antonopoulos, L. Angquist, and H.-P. Nee, "On dynamics and voltage control of the modular multilevel converter," in *13th European Conference on Power Electronics and Applications, 2009. EPE '09*, Sep. 2009, pp. 1–10.
[29] S. Samimi, F. Gruson, P. Delarue, F. Colas, M. M. Belhaouane, and X. Guillaud, "MMC stored energy participation to the DC bus voltage control in an HVDC link," *IEEE Transactions on Power Delivery*, vol. 31, no. 4, pp. 1710–1718, Aug. 2016.

**Haibo Zhang** received the B.Sc. degree from Shanghai Maritime University, China in 2012, and the M.Sc. degree from Université de Nantes, France in 2014. In 2017, he obtained his Ph.D degree on Electrical Engineering from Université des Sciences et Technologies de Lille, France. Since 2018, he has been a postdoctoral researcher in the Laboratoire d'Electrotechnique et d'Electronique de Puissance of Lille (L2EP), Ecole Centrale de Lille, Villeneuve d'Ascq, France. His research interests include control and modeling of power electronic converter and hardware-in-the loop simulation.

**François Gruson** received the Ph.D. degree in electrical engineering from the Ecole Centrale de Lille, Lille, France, in 2010. Since 2011, he has been an Associate Professor in the Laboratoire d'Electrotechnique et d'Electronique de Puissance of Lille, Arts and Metiers ParisTech, Lille, France. His research interests include power electronic converter and power quality for distribution and transmission grid applications and especially for HVdc transmission grid.

**Diana M. Flórez Rodriguez** received the Electrical Engineering degree from National University of Colombia, Manizales, and the M.Sc. and Ph.D degrees in Electrical Engineering, Electronics and Automation from University Carlos III of Madrid, Spain, in 2006, 2008 and 2012, respectively. She is currently an Associate professor with Ecole des Hautes Etudes d'Ingénieur, France after a Postdoctoral training in the field of Reliability Assessment of Wind Farms at Ecole Centrale de Lille, at the Laboratoire d'Electrotechnique et d'Electronique de Puissance of Lille, France. She deals with modeling, analysis and control of wind energy conversion systems, the integration of renewable energy generation systems into electrical grids and smart grids.

**Christophe Saudemont** received the Ph.D. degree in electrical engineering from the University of Sciences and Technologies of Lille, Lille, France, in 1999. Since 2001, he has been with the Department of Electrical Engineering, Ecole des Hautes Etudes d'Ingénieur, Lille, and since 2002, he has also been a researcher with the Laboratoire d'Electrotechnique et d'Electronique de Puissance of Lille, Lille. His work is focused on the renewable energies, decentralized electric energy production and integration of dispersed renewable energy sources, and smart grids. Dr. Saudemont is a member of the "Société Française des Electriciens et des Electroniciens" (SEE).